

2015

# Thermal stability and properties of deformation-processed Cu-Fe in situ composites

Keming Liu
*University of Wollongong*, keming@uow.edu.au

Zhengyi Jiang
*University of Wollongong*, jiang@uow.edu.au

Jingwei Zhao
*University of Wollongong*, jzhao@uow.edu.au

Jin Zou
*Jiangxi Academy of Sciences*

Lei Lu
*University of Wollongong*, ll490@uowmail.edu.au

***See next page for additional authors***

## Publication Details

Liu, K., Jiang, Z., Zhao, J., Zou, J., Lu, L. & Lu, D. (2015). Thermal stability and properties of deformation-processed Cu-Fe in situ composites. Metallurgical and Materials Transactions A: Physical Metallurgy and Materials Science, 46 (5), 2255-2261.

# Thermal stability and properties of deformation-processed Cu-Fe in situ composites

**Abstract**
This paper investigated the thermal stability, tensile strength, and conductivity of deformation-processed Cu-14Fe in situ composites produced by thermo-mechanical processing. The thermal stability was analyzed using scanning electronic microscope and transmission electron microscope. The tensile strength and conductivity were evaluated using tensile-testing machine and micro-ohmmeter, respectively. The Fe fibers in the deformation-processed Cu-14Fe in situ composites undergo edge recession, longitudinal splitting, cylinderization, break-up, and spheroidization during the heat treatment. The Cu matrix experiences recovery, recrystallization, and precipitation phase transition. The tensile strength and conductivity first increase with increasing temperature of heat treatment, reach peak values at different temperatures, and then decrease at higher temperatures. The value of parameter Z of the in situ composite reaches the peak of 2.86 x 107 MPa2 pct IACS after isothermal heat treatment at 798 K (525 °C) for 1 hour. The obtained tensile strength and conductivity of the in situ composites are 907 MPa and 54.3 pct IACS; 868 MPa and 55.2 pct IACS; 810 MPa and 55.8 pct IACS; or 745 MPa and 57.4 pct IACS, at $\eta = 7.8$ after isochronal heat treatment for 1 hour.

**Keywords**
properties, deformation, processed, thermal, cu, stability, fe, situ, composites

**Disciplines**
Engineering | Science and Technology Studies

**Publication Details**
Liu, K., Jiang, Z., Zhao, J., Zou, J., Lu, L. & Lu, D. (2015). Thermal stability and properties of deformation-processed Cu-Fe in situ composites. Metallurgical and Materials Transactions A: Physical Metallurgy and Materials Science, 46 (5), 2255-2261.

**Authors**
Keming Liu, Zhengyi Jiang, Jingwei Zhao, Jin Zou, Lei Lu, and Deping Lu

# Thermal Stability and Properties of Deformation-Processed Cu-Fe *In Situ* Composites

KEMING LIU, ZHENGYI JIANG, JINGWEI ZHAO, JIN ZOU, LEI LU, and DEPING LU

This paper investigated the thermal stability, tensile strength, and conductivity of deformation-processed Cu-14Fe *in situ* composites produced by thermo-mechanical processing. The thermal stability was analyzed using scanning electronic microscope and transmission electron microscope. The tensile strength and conductivity were evaluated using tensile-testing machine and micro-ohmmeter, respectively. The Fe fibers in the deformation-processed Cu-14Fe *in situ* composites undergo edge recession, longitudinal splitting, cylinderization, break-up, and spheroidization during the heat treatment. The Cu matrix experiences recovery, recrystallization, and precipitation phase transition. The tensile strength and conductivity first increase with increasing temperature of heat treatment, reach peak values at different temperatures, and then decrease at higher temperatures. The value of parameter $Z$ of the *in situ* composite reaches the peak of $2.86 \times 10^7$ MPa$^2$ pct IACS after isothermal heat treatment at 798 K (525 °C) for 1 hour. The obtained tensile strength and conductivity of the *in situ* composites are 907 MPa and 54.3 pct IACS; 868 MPa and 55.2 pct IACS; 810 MPa and 55.8 pct IACS; or 745 MPa and 57.4 pct IACS, at $\eta = 7.8$ after isochronal heat treatment for 1 hour.

DOI: 10.1007/s11661-015-2791-x


## I. INTRODUCTION

BINARY deformation-processed Cu-Fe *in situ* composites produced by thermo-mechanical processing have been the subject of extensive research during the past two decades due to the low cost of iron.[1–9] However, the Cu-Fe system *in situ* composites have relatively low conductivity because of the relatively high solubility of Fe in Cu at high temperatures, the slow kinetics of Fe precipitation at lower temperatures, and the particularly harmful influence of iron atoms in solid solution on the conductivity.[10,11] Previous research[12,13] has explored two main approaches to improve the strength and conductivity of Cu-based systems *in situ* composites. One approach is to modify the composition, particularly using extra alloying elements.[14–16] Ag has been used as a third element in many studies,[17–23] because the electronegativity, electronic structure, and crystal structure of Ag are similar to those of Cu and the electrical conductivity of Ag is higher than that of Cu. The other approach is to modify the processing using various heat treatments.

Heat treatment with appropriate holding time and temperature allows high conductivity to be achieved and can produce an excellent combination of strength and conductivity.[24–28] Raabe and Ge[19] investigated the effect of annealing temperature and time on the microstructure of Cu-10Cr-3Ag *in situ* composite, and found that the fibers underwent a capillarity-driven shape change from bamboo morphology with grain boundary grooves to complete spheroidization during annealing. Stepped annealing process for Cu-11Fe-6Ag and Cu-12Fe *in situ* composites was investigated by Gao *et al.*[29] They found that proper stepped annealing at a certain draw ratio produced better combination of strength and conductivity. The work of Xie *et al.*[5] indicated that the prior homogenization heat treatment resulted in the refinement of the primary Fe dendrites in the Cu matrix and promoted the precipitation of the secondary Fe particles from the Cu matrix, which led to an increase in the strength and conductivity of the *in situ* composites. The result obtained by Wu *et al.*[30] showed that heat treatments could improve the strength of Cu-6 wt pct Fe and Cu-12 wt pct Fe filamentary composites by increasing the precipitation strengthening and interface strengthening levels.

In our previous work,[10] we investigated the microstructure and properties of deformation-processed Cu-14Fe *in situ* composite produced by thermo-mechanical processing. This paper builds on that work and studies the influence of heat treatments on the microstructure and properties of deformation-processed Cu-14Fe *in situ* composites with the purpose of producing a Cu-Fe *in situ* composite with excellent combination of tensile strength and electrical conductivity.

KEMING LIU, Associate Professor, is with the Jiangxi Key Laboratory for Advanced Copper and Tungsten Materials, Jiangxi Academy of Sciences, Nanchang 330029, P.R. China, and also with the School of Mechanical, Materials and Mechatronic Engineering, University of Wollongong, Wollongong, NSW 2522, Australia. Contact e-mail: jokeyliu@163.com ZHENGYI JIANG, Professor, and JINGWEI ZHAO, Research Fellow, are with the School of Mechanical, Materials and Mechatronic Engineering, University of Wollongong. Contact e-mail: jiang@uow.edu.au JIN ZOU, Research Assistant, LEI LU and DEPING LU, Professors, are with the Jiangxi Key Laboratory for Advanced Copper and Tungsten Materials, Jiangxi Academy of Sciences.

Manuscript submitted October 7, 2014.



Published online: 11 February 2015

## II. EXPERIMENTAL DETAILS

The Cu-14Fe alloy was prepared by melting appropriate amounts of electrolytic Cu, commercial Fe (of at least 99.94 wt pct purity) in a magnesia crucible using a vacuum induction furnace, and then was casted into a rod-shaped ingot of about 36 mm in diameter using a graphite mold. The *in situ* composite was produced by thermo-mechanical processing as follows. The rod-shaped ingot was heated to 1223 K (950 °C) at a rate of 5 K/min, held for 3 hours and then water quenched. The quenched ingot was hot rolled at 1123 K (850 °C) and machined to remove surface oxides and defects. The machined ingot was heated to 1223 K (950 °C) at a rate of 5 K/min, held for 70 minutes and then water quenched. The quenched ingot was cold drawn to a cumulative cold deformation strain of $\eta = 7$ and was cut into heat-treated samples. Then they were subjected to isochronal heat treatments for 1 hour at different temperatures from 473 K to 973 K (200 °C to 700 °C) and isothermal heat treatments at 798 K (525 °C) for different times from 1 to 8 hours, and finally furnace cooled to room temperature. The heat-treated sample was cold drawn to $\eta = 7.8$, and aged by heating to temperatures from 473 K to 873 K (200 °C to 600 °C) for 1 hour, and finally furnace cooled to room temperature. The heating rate is 5 K/min. The cumulative cold deformation strain was obtained by

$$\eta = \ln(A_0/A_f), \quad [1]$$

where $A_0$ is the original cross-sectional area and $A_f$ is the final cross-sectional area.

The microstructures of the deformation-processed and heat-treated samples were investigated using a scanning electronic microscope (SEM) and a transmission electronic microscope (TEM). The SEM specimens were prepared through mounting, mechanical grinding, polishing, and then etching in a solution of 120 mL $H_2O$, 20 mL HCl, and 5 g $FeCl_3$. The TEM specimens were prepared by mechanical thinning using grinding papers, decreasing the thickness using a dimple machine, and ion milling using a Gatan Model 600 ion beam thinner. The tensile properties of the deformation-processed and heat-treated specimens were evaluated using an electronic tensile-testing machine. The ultimate tensile stress (UTS) was taken as a measure of the tensile strength for comparison purposes because it was very reproducible and well defined for similar specimens. The electrical resistivity ($\rho$) was measured by a ZY9987 digital micro-ohmmeter with precision of 1 $\mu\Omega$ at room temperature. The corresponding conductivity was evaluated according to the definition of International Annealed Copper Standard (IACS) in which 1.7241 $\mu\Omega$·cm is defined as 100 pct IACS.

## III. RESULTS AND DISCUSSION

### A. *Thermal Stability*

Figure 1 presents the SEM microstructures of the Cu-14Fe *in situ* composite with $\eta = 7$ in the longitudinal section, heat treated for 1 hour at different temperatures ranging from 573 K to 873 K (300 °C to 600 °C). The microstructure of the as-drawn *in situ* composite is composed of Cu matrix and elongated Fe fibers. The darker fibers correspond to the Fe phase, and the lighter areas correspond to the Cu matrix. At temperatures lower than 573 K (300 °C), no pronounced change in the morphology of the Fe fibers is observed, as shown in Figure 1(a). At the temperature of 673 K (400 °C), edge recessions and thermal grooves in Fe phase are occasionally found in the longitudinal section although the interfaces between Cu matrix and Fe fibers are still clear, as seen in Figure 1(b). At the temperature of 773 K (500 °C), obvious unevenness of the fibers surface and coarsening can be observed, and some fibers are starting longitudinal splitting and cylinderization, as observed in Figure 1(c). With the further increase of temperature, the break-up and spheroidization of the Fe fibers start to take place. At the temperature of 873 K (600 °C), break-up and spheroidization are seen distinctly in most of the fibers, and some fine fibers are transformed into sphere chains, as shown in Figure 1(d). The Fe fibers experience morphology changes such as edge recession, longitudinal splitting, cylinderization, break-up, and spheroidization after exposed to elevated temperatures, which is in agreement with previous research.[19,28]

Figure 2 presents the TEM images of the Cu-14Fe *in situ* composite with $\eta = 7$ heat treated for 1 hour at different temperatures ranging from 573 K to 873 K (300 °C to 600 °C). At temperatures lower than 573 K (300 °C), recovery occurs in most of the Cu grains and there are no pronounced precipitates, but elongated cellular substructures parallel to the drawing direction can be observed, and lots of dislocations are found in the cell walls of the substructure, as indicated by the arrows in Figure 2(a). At the temperature of 673 K (400 °C), subgrain boundaries are clear because of the dislocation climb, crystallization nucleus can be observed in the junction of subgrains and the interior of the Cu grains with high energy, as indicated by the arrows in Figure 2(b), and some grains' crystallizations have completed. With the further increase of temperature, recrystallization and precipitation proceed simultaneously in the Cu matrix. At the temperature of 773 K (500 °C), precipitates can be seen obviously in the recrystallized grains, as indicated by the arrows in Figure 2(c). However, even though at the temperature of 873 K (600 °C), subgrains are still visible in some grains, as indicated by the arrows in Figure 2(d), which suggests that the migration of Cu grain boundaries is immensely impeded and continuous recrystallization accompanied with discontinuous recrystallization during the heat treatment. Gao *et al.*[28] studied the thermal stability of deformation-processed Cu-Fe *in situ* composite and found the similar changes in the Cu matrix of Cu-12Fe *in situ* composite during annealing treatment. As shown in Figure 2, there are two main changes in the Cu matrix during the heat treatment. One change is the recovery and recrystallization, and the other change is the precipitation of the supersaturated Cu matrix.

### B. *Strength and Conductivity*

Figure 3 presents the tensile strength and conductivity of the Cu-14Fe *in situ* composite with $\eta = 7$ heat treated

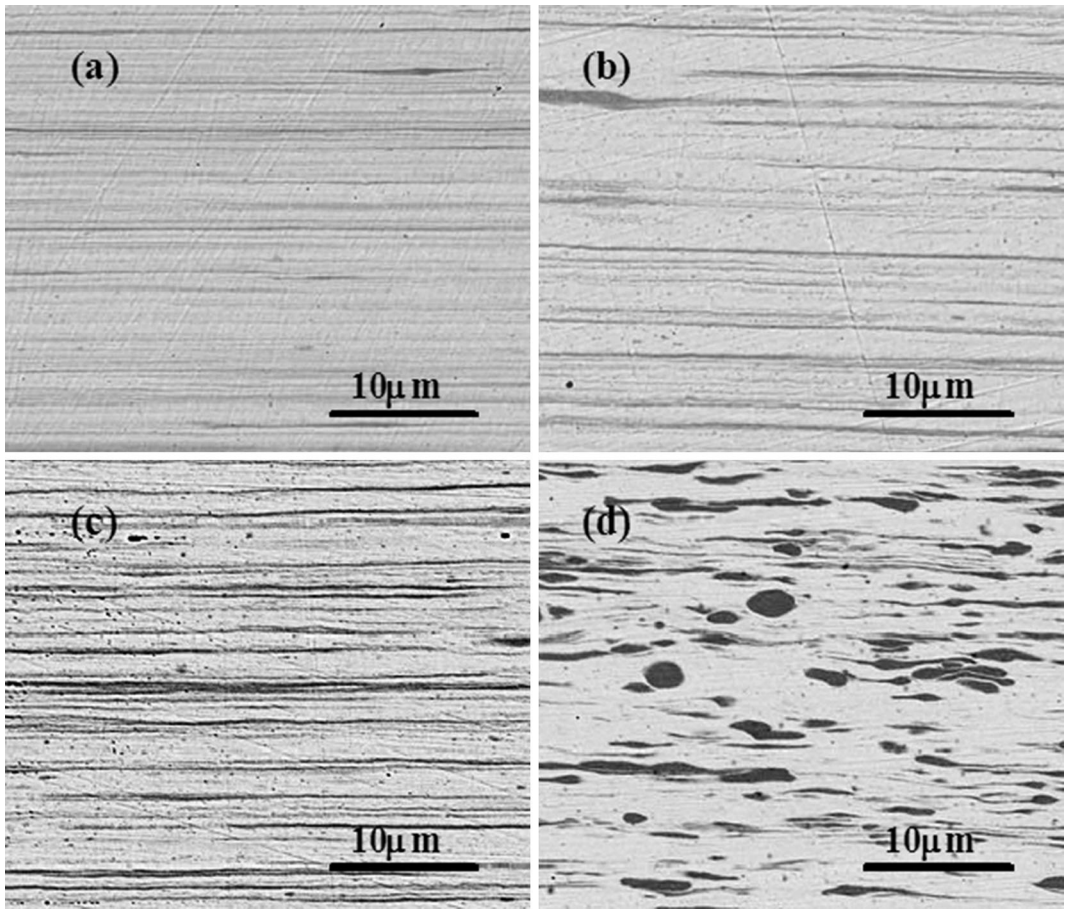


Fig. 1—Longitudinal SEM microstructures of Cu-14Fe *in situ* composite at $\eta = 7$ after heat treatment at different temperatures for 1 h: (*a*) 573 K (300 °C), (*b*) 673 K (400 °C), (*c*) 773 K (500 °C), and (*d*) 873 K (600 °C).

for 1 hour at different temperatures ranging from 473 K to 973 K (200 °C to 700 °C). As shown in Figure 3, both the tensile strength and conductivity of the *in situ* composite increase gradually after isochronal aging treatment. The tensile strength reaches a peak value at 673 K (400 °C), and then it is progressively lower after isochronal heat treatments at higher temperatures. At temperatures lower than 673 K (400 °C), there is no significant coarsening of Fe fibers by recrystallization, whereas some fine Fe precipitates increase the strength of the Cu matrix. Gao *et al.*[27] reported that the precipitation strengthening of nano-scaled Fe particles led to the formation of the hardness peak of Cu-12Fe *in situ* composite. At higher temperatures, the tensile strength decreases because the heat treatment promotes the coarsening of Fe fibers, the conglomeration of precipitated Fe particles, the recovery, and recrystallization of the Cu matrix.[1,10,27] Similar to the effect of different heat treatments on the tensile strength, the conductivity reaches a peak at 798 K (525 °C), and then it is progressively lower after isochronal heat treatments at higher temperatures. The increase in conductivity to 798 K (525 °C) is attributed to the decrease of Fe atoms in solid solution in the Cu matrix.[1] At higher temperatures, the coarsening of Fe fibers induces much more cross-sectional Cu/Fe phase interfaces and the conduction is forced to penetrate through the highly resistive Fe phase, which results in a rapid decrement of conductivity. Furthermore, the high solubility of Fe in the Cu matrix above 798 K (525 °C) can also contribute to the conductivity drop.[1,27]

### C. *Determination of Heat Treatment Process*

Figure 4 presents the tensile strength and conductivity of the Cu-14Fe *in situ* composite with $\eta = 7$ heat treated at 798 K (525 °C) for different times ranging from 1 to 8 hours. As mentioned above, the tensile strength and conductivity of the Cu-14Fe *in situ* composite increase with the heat treatment temperature and reaches the peak value at 673 K and 798 K (400 °C and 525 °C), respectively. At temperatures higher than 798 K (525 °C), the tensile strength and conductivity reduce at a high rate of speed. Therefore, the proper heat treatment temperature should not exceed 798 K (525 °C). In addition, the tensile strength can be rapidly improved through a subsequent cold deformation. For this reason, 798 K (525 °C) is selected as the isothermal heat treatment temperature. As shown in Figure 4, the tensile strength of the *in situ* composite reduces after isothermal heat treatment, and the decrement increases with increasing time of isothermal heat treatment. The conglomeration of the precipitated particles and the coarsening of the fibers intensify, and the recrystalliza-

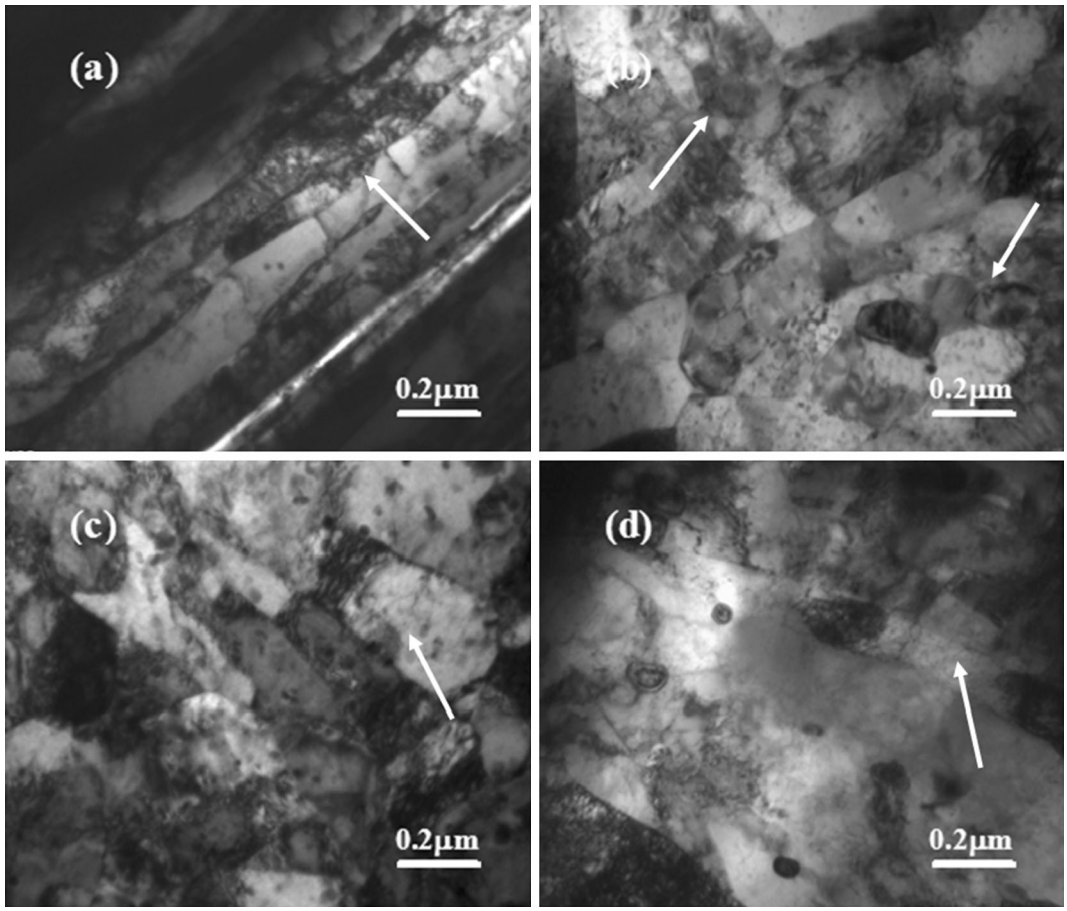


Fig. 2—TEM microstructures of Cu-14Fe *in situ* composite at $\eta = 7$ after heat treatment at different temperatures for 1 h: (*a*) 573 K (300 °C), (*b*) 673 K (400 °C), (*c*) 773 K (500 °C), and (*d*) 873 K (600 °C).

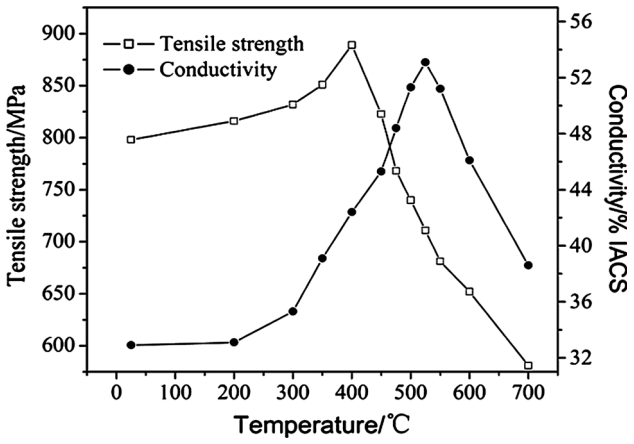


Fig. 3—Tensile strength and conductivity curves of Cu-14Fe *in situ* composites at $\eta = 7$ after isochronal heat treatment for 1 h.

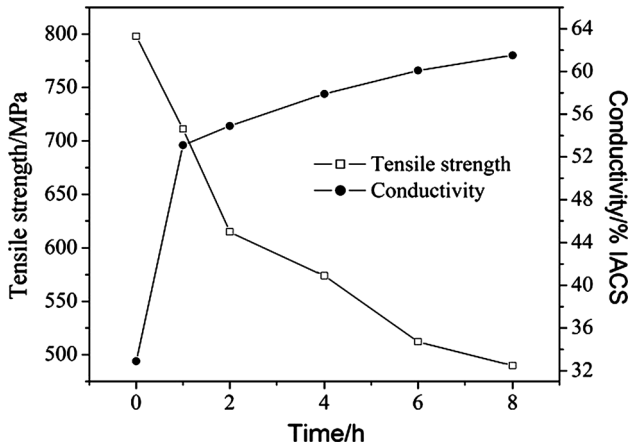


Fig. 4—Tensile strength and conductivity curves of Cu-14Fe *in situ* composites at $\eta = 7$ after isothermal heat treatment at 798 K (525 °C).

tion of the matrix is more sufficient with increasing time of isothermal heat treatment, which decreases the tensile strength of the *in situ* composite. Different from the change of the tensile strength, the conductivity of the *in situ* composite rises after isothermal heat treatment. The increment increases with increasing time of isothermal heat treatment. The Fe atoms in solid solution in the Cu matrix reduces with increasing time of isothermal heat treatment, and the break-up and spheroidization of the Fe fibers hardly occur after heat treatments at 798 K (525 °C) for different times used in this investigation, which promotes the increase of conductivity. This finding is in agreement with previous research.[10,29]

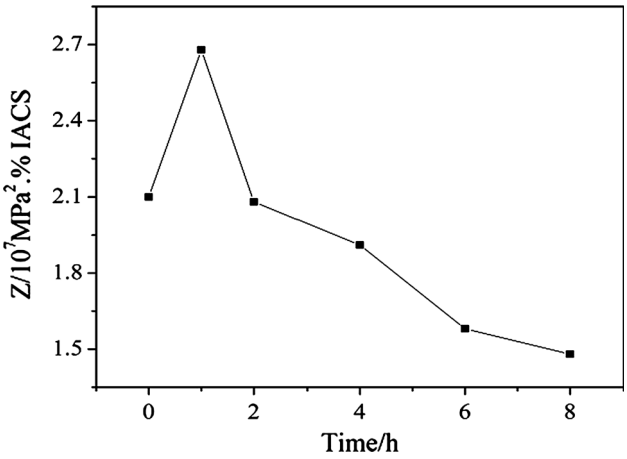


Fig. 5—$Z$ value curve of Cu-14Fe *in situ* composites at $\eta = 7$ after isothermal heat treatment at 798 K (525 °C).

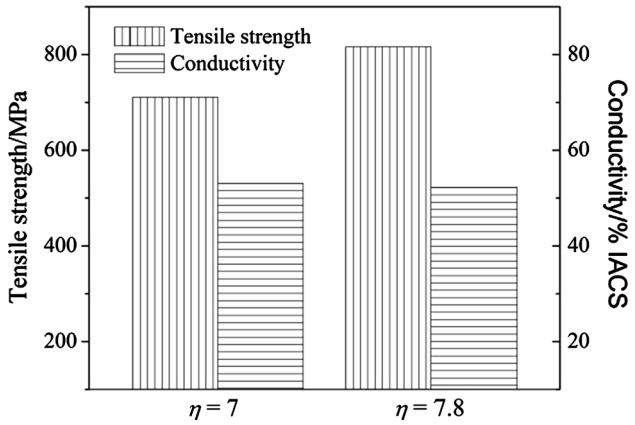


Fig. 6—Tensile strength and conductivity of Cu-14Fe *in situ* composite with $\eta = 7$ after 798 K (525 °C) × 1 h heat treatment, and cold drawing to $\eta = 7.8$ after heat treatment at $\eta = 7$.

Figure 5 presents $Z$ value curve of the Cu-14Fe *in situ* composites with $\eta = 7$ heat treated at 798 K (525 °C) for different times ranging from 1 to 8 h. As mentioned above, the conductivity of the Cu-14Fe *in situ* composite increases, while the tensile strength decreases with increasing time of heat treatment. Any of the two properties cannot represent the service performance of the *in situ* composite. Based on lots of running tests of electric railway contact wires, a parameter $Z$ evaluated that the combination property of Cu-based *in situ* composites is proposed in Japan. The parameter can be expressed as follows[29,31]:

$$Z = \sigma_b^2 \times \varphi, \qquad [2]$$

where $\sigma_b$ is the tensile strength and $\varphi$ is the electrical conductivity of the composites. As shown in Figure 5, the value of parameter $Z$ of the *in situ* composite increases after isothermal heat treatment at 798 K (525 °C) and reaches a peak value at 1 hour, then the $Z$ value is progressively lower after isothermal heat treatments at longer time, which indicates that the optimum combination property can be obtained when the *in situ* composite is heat treated at 798 K (525 °C) for 1 hour. Therefore, 798 K (525 °C) and 1 hour are, respectively, selected as the optimum heat treatment temperature and duration time for the *in situ* composite.

### D. *Final Combination of Strength and Conductivity*

Figure 6 presents the conductivity and tensile strength of the Cu-14Fe *in situ* composites with $\eta = 7$ after heat treatment at 798 K (525 °C) for 1 hour and cold drawing to $\eta = 7.8$ after heat treatment at $\eta = 7$, respectively. As shown in Figure 6, the conductivity of the *in situ* composite after heat treatment at $\eta = 7$ drops slightly, and the tensile strength rapidly improves after cold drawing to $\eta = 7.8$. The resistivity of the deformation-processed Cu-based *in situ* composites is dependent on the parallel circuit model,[10,15,21,27] which suggests about 97 pct resistivity of Cu-Fe *in situ* composite results from the Cu matrix,[27] and the resistivity of the Cu matrix can be partitioned into the contribution of four principal scattering mechanisms, *i.e.*, interface, phonon, dislocation, and impurity scattering. In addition, previous research[21,27] indicated that the strength of deformation-processed Cu-based *in situ* composites obeys the Hall–Petch equation, *i.e.*, $\sigma \propto \lambda^{-1/2}$, where $\sigma$ is the tensile strength of Cu-based *in situ* composites and $\lambda$ is the fiber spacing. As a result, the electrical conductivity and tensile strength of the deformation-processed Cu-based *in situ* composites are mainly determined by the microstructures.

Figure 7 presents the SEM microstructures of the Cu-14Fe *in situ* composite with $\eta = 7$ after heat treatment at 798 K (525 °C) for 1 hour and $\eta = 7.8$ in the longitudinal sections. Figure 7(a) indicates that the fibers' surfaces are strongly uneven and the fibers become significant coarsen in the *in situ* composite after heat treatment. While the uneven and coarsening fibers are renewedly transformed into uniform and fine fibers by being further cold drawn to $\eta = 7.8$, as shown in Figure 7(b). This result suggests that the morphology changes of the fibers in deformation-processed *in situ* composites can be rapidly refined and homogenized through a subsequent cold deformation. Further cold deformation promotes the refining and homogenization of the uneven and coarsening fibers in the *in situ* composite, and will decrease the fiber spacing and increase the interface density. The tensile strength rapidly rises after cold drawing to $\eta = 7.8$ due to the decrease of fiber spacing. The conductivity slightly drops after cold drawing to $\eta = 7.8$ because the increased interface density improved interface scattering resistivity, which indicates that selecting the temperature of the conductivity peak value as the optimum heat treatment temperature is reasonable.

Figure 8 presents the tensile strength and conductivity of the Cu-14Fe *in situ* composite with $\eta = 7.8$ heat treated for 1 hour at different temperatures ranging from 473 K to 873 K (200 °C to 600 °C), respectively. As mentioned above, the parameter $Z$ reaches a peak value after heat treatment for 1 hour. The tensile strength and conductivity of the *in situ* composite increase gradually with increasing temperature of heat

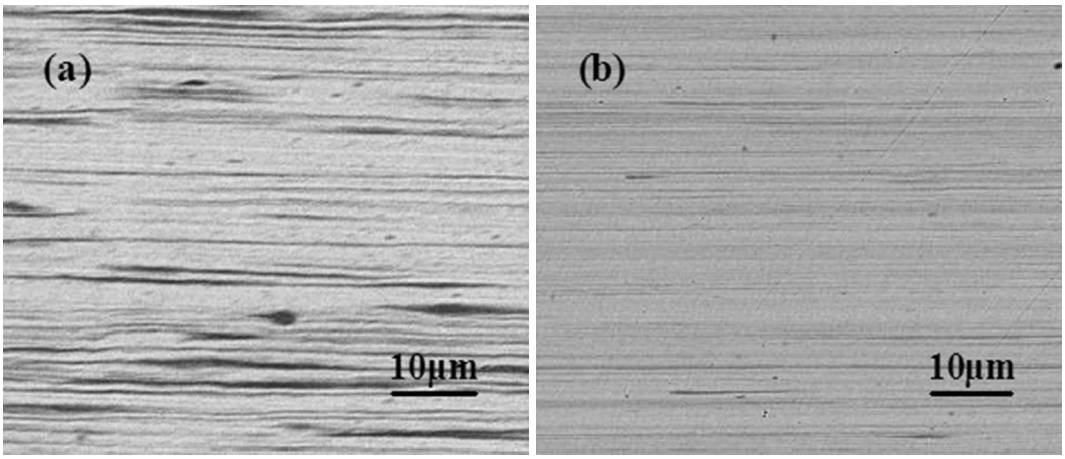


Fig. 7—SEM microstructures of Cu-14Fe *in situ* composites: (*a*) 798 K (525 °C) × 1 h heat treatment at $\eta = 7$, and (*b*) cold drawing to $\eta = 7.8$ after 798 K (525 °C) × 1 h heat treatment at $\eta = 7$.

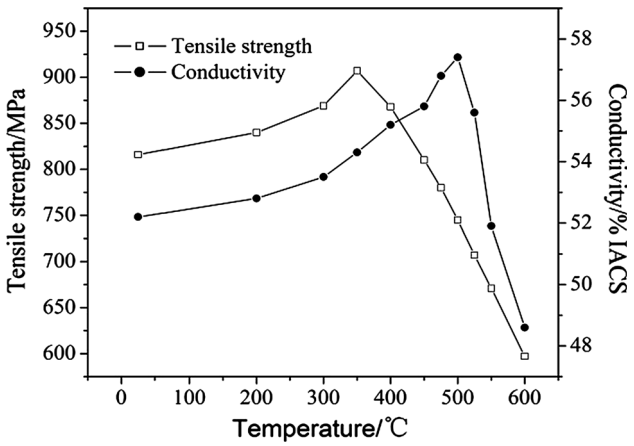


Fig. 8—Tensile strength and conductivity of Cu-14Fe *in situ* composite at $\eta = 7.8$ *vs* aging temperature of isochronal heat treatment for 1 h.

treatment and reach peak values at different temperatures, and then both values decrease at higher temperatures. Therefore, aging for 1 hour at different temperatures is selected as the heat treatment process to adjust and control the strength and conductivity of the deformation-processed Cu-14Fe *in situ* composite with $\eta = 7.8$. As shown in Figure 8, similar to the influence of heat treatment on the Cu-14Fe *in situ* composite with $\eta = 7$, the tensile strength and conductivity of the Cu-14Fe *in situ* composite with $\eta = 7.8$ first increase and then decrease with increasing temperature of aging treatment. While the temperatures of the tensile strength and conductivity peak of the *in situ* composite at $\eta = 7.8$ heat treated for 1 hour are, respectively, lower than those of the *in situ* composite at $\eta = 7$. This is attributed to the fact that the heat stability of Cu-14Fe *in situ* composite at $\eta = 7.8$ is weaker than that at $\eta = 7$.[1,27,32] The tensile strength and conductivity of the deformation-processed Cu-14Fe *in situ* composite with $\eta = 7.8$ after isochronal heat treatment for 1 hour reach 907 MPa and 54.3 pct IACS; 868 MPa and 55.2 pct IACS; 810 MPa and 55.8 pct IACS; or 745 MPa and 57.4 pct IACS.

## IV. CONCLUSIONS

1. The Fe fibers in the deformation-processed Cu-14Fe *in situ* composites undergo morphology changes such as edge recession, longitudinal splitting, cylinderization, break-up, and spheroidization after exposure to elevated temperatures.
2. The Cu matrix experiences recovery, recrystallization, and precipitation phase transition during the heat treatment.
3. The tensile strength and conductivity first increase with increasing temperature of heat treatment, reach peak values at different temperatures, and then decrease at higher temperatures.
4. The value of parameter $Z$ of the deformation-processed Cu-14Fe *in situ* composite with $\eta = 7$ after the isothermal heat treatments at 798 K (525 °C) for 1 hour reaches the peak value of $2.86 \times 10^7$ MPa$^2$ pct IACS.
5. The tensile strength and conductivity of the deformation-processed Cu-14Fe *in situ* composite with $\eta = 7.8$ after isochronal heat treatment for 1 hour reach 907 MPa and 54.3 pct IACS; 868 MPa and 55.2 pct IACS; 810 MPa and 55.8 pct IACS; or 745 MPa and 57.4 pct IACS.

## ACKNOWLEDGMENTS

This project was supported by the National Natural Science Foundation of China (51461018), the China Scholarship Council (2011836024), the Key Program of Natural Science Foundation of Jiangxi Province (20133BAB20008; 20144ACB20013), the Science and Technology Support Plan of Jiangxi Province (20123BBE50112), and the Key Science and Tech-

nology Program of Jiangxi Province Bureau of Quality and Technical Supervision (ZJKJ2013003).

## REFERENCES


1. K.M. Liu, D.P. Lu, H.T. Zhou, Z.B. Chen, A. Atrens, and L. Lu: *Mater. Sci. Eng. A*, 2013, vol. 584, pp. 114–20.
2. Z.X. Xie, H.Y. Gao, S.J. Dong, J. Wang, H. Huang, and P. Luo: *Mater. Trans.*, 2013, vol. 54, pp. 2075–78.
3. J.P. Ge, H. Zhao, Z.Q. Yao, and S.H. Liu: *Trans. Nonferrous Met. Soc. China*, 2005, vol. 15, pp. 971–77.
4. Z.W. Wu, J.J. Liu, Y. Chen, and L. Meng: *J. Alloys Compd.*, 2009, vol. 467, pp. 213–18.
5. Z.X. Xie, H.Y. Gao, J. Wang, and B.D. Sun: *Mater. Sci. Eng. A*, 2011, vol. 529, pp. 388–92.
6. H. Fernee, J. Nairn, and A. Atrens: *J. Mater. Sci.*, 2001, vol. 36, pp. 2711–19.
7. J.S. Song and S.I. Hong: *J. Alloys Compd.*, 2000, vol. 311, pp. 265–69.
8. Y.S. Kim, J.S. Song, and S.I. Hong: *J. Mater. Proc. Technol.*, 2002, vols. 130–131, pp. 278–82.
9. S.I. Hong, J.S. Song, and H.S. Kim: *Scripta Mater.*, 2001, vol. 45, pp. 1295–1300.
10. K.M. Liu, D.P. Lu, H.T. Zhou, A. Atrens, J. Zou, Y.L. Yang, and S.M. Zeng: *Mater. Sci. Eng. A*, 2010, vol. 527, pp. 4953–58.
11. B. Sun, H. Gao, J. Wang, and D. Shu: *Mater. Lett.*, 2007, vol. 61, pp. 1002–06.
12. Y. Jin, K. Adachi, T. Takeuchi, and H.G. Suzuki: *J. Mater. Sci.*, 1998, vol. 33, pp. 1333–41.
13. H. Gao, J. Wang, D. Shu, and B. Sun: *Scripta Mater.*, 2005, vol. 53, pp. 1105–09.
14. J.Q. Deng, X.Q. Zhang, S.Z. Shang, F. Liu, Z.X. Zhao, and Y.F. Ye: *Mater. Des.*, 2009, vol. 30, pp. 4444–49.
15. J.S. Song, H.S. Kim, C.T. Lee, and S.I. Hong: *J. Mater. Proc. Technol.*, 2002, vols. 130–131, pp. 272–77.
16. J.S. Song, S.I. Hong, and H.S. Kim: *J. Mater. Proc. Technol.*, 2001, vol. 113, pp. 610–16.
17. D. Raabe, S. Ohsaki, and K. Hono: *Acta Mater.*, 2009, vol. 57, pp. 5254–63.
18. K.M. Liu, D.P. Lu, H.T. Zhou, A. Atrens, Z.B. Chen, J. Zou, and S.M. Zeng: *J. Alloys Compd.*, 2010, vol. 500, pp. L22–25.
19. D. Raabe and J. Ge: *Scripta Mater.*, 2004, vol. 51, pp. 915–20.
20. Y. Liu, S. Shao, K.M. Liu, X.J. Yang, and D.P. Lu: *Mater. Sci. Eng. A*, 2012, vol. 531, pp. 141–46.
21. K.M. Liu, D.P. Lu, H.T. Zhou, Y.L. Yang, A. Atrens, and J. Zou: *J. Mater. Eng. Perform.*, 2013, vol. 22, pp. 3723–27.
22. Z.X. Xie, H.Y. Gao, Q. Lu, J. Wang, and B.D. Sun: *J. Alloys Compd.*, 2010, vol. 508, pp. 320–23.
23. J.S. Song, S.I. Hong, and Y.G. Park: *J. Alloys Compd.*, 2005, vol. 388, pp. 69–74.
24. J.D. Klein and R.M. Rose: *J. Appl. Phys.*, 1990, vol. 67, pp. 930–34.
25. J.S. Carpenter, R.J. Mccabe, S.J. Zheng, T.A. Wynn, N.A. Mara, and I.J. Beyerlein: *Metall. Mater. Trans. A*, 2014, vol. 45A, pp. 2192–2208.
26. L. Qu, E. Wang, K. Han, X. Zuo, L. Zhang, P. Jia, and J. He: *J. Appl. Phys.*, 2013, vol. 113, p. 173708.
27. H. Gao, J. Wang, D. Shu, and B. Sun: *Scripta Mater.*, 2006, vol. 54, pp. 1931–35.
28. H. Gao, J. Wang, and B. Sun: *J. Alloys Compd.*, 2009, vol. 469, pp. 580–86.
29. H. Gao, J. Wang, D. Shu, and B. Sun: *J. Alloys Compd.*, 2007, vol. 438, pp. 268–73.
30. Z.W. Wu and L. Meng: *J. Alloys Compd.*, 2011, vol. 509, pp. 8917–21.
31. L.M. Peng, X.M. Mao, K.D. Xu, and W.J. Ding: *J. Mater. Proc. Technol.*, 2005, vol. 166, pp. 193–98.
32. K.M. Liu, Z.Y. Jiang, J.W. Zhao, J. Zou, Z.B. Chen, and D.P. Lu: *J. Alloys Compd.*, 2014, vol. 612, pp. 221–26.